



Contents lists available at ScienceDirect

Arabian Journal of Chemistry

journal homepage: www.sciencedirect.com



Original article

Anti-hyperlipidemic and antioxidant ability of HeShouWu (roots of *Polygonum multiflorum* Thunb.) and its complex formulaPing-Hsiu Huang^{a,1}, Yu-Tsung Cheng^{b,c,1}, Yung-Jia Chan^d, Shu-Ju Chen^c, Jhih-Ying Ciou^e, Wen-Chien Lu^f, Wan-Jung Hsu^c, Chiun-Chung R. Wang^c, Po-Hsien Li^{c,*}^a School of Food, Jiangsu Food and Pharmaceutical Science College, Huai'an, Jiangsu Province 223003, China^b Cardiovascular Center, Taichung Veterans General Hospital, Taichung 40705, Taiwan^c Department of Food and Nutrition, Providence University, Taichung City 43301, Taiwan^d College of Biotechnology and Bioresources, Da-Yeh University, Changhua 51591, Taiwan^e Department of Food Science, Tunghai University, Taichung City 40704, Taiwan^f Department of Food and Beverage Management, Chung-Jen Junior College of Nursing, Health Sciences and Management, Chia-Yi City 60077, Taiwan

ARTICLE INFO

Article history:

Received 7 April 2023

Accepted 16 September 2023

Available online 21 September 2023

Keywords:

HeShouWu (roots of *Polygonum multiflorum*)

Blood lipids

Triglycerides

Total cholesterol

Low-cholesterol diet

Chinese herbal formulations

ABSTRACT

Many studies have confirmed the effectiveness of herbal medicines or complex formulations in clinical therapy for metabolic diseases. This study investigated the effects of a HeShouWu decoction and its complex formula on blood lipids and antioxidant activity in hamsters with a high-cholesterol intake-induced hyperlipidemia model. The biological efficacy of HeShouWu and its complex formula were assessed by measuring body weight (BW), and fecal metabolites, conducting a blood biochemical analysis, and examining liver sections. Triglycerides (TG), total cholesterol (TC) contents, and antioxidant activities in the liver and kidneys were measured. The results showed no inhibited growth after 10 weeks of treatment. However, significant decreases in blood and liver lipids (TC and TG) were detected in all treatment groups ($p < 0.05$). Moreover, the antioxidant activities [glutathione peroxidase (GSH-Px), superoxide dismutase (SOD), catalase (CAT), and total thiols] improved, and malondialdehyde (MDA) content decreased significantly, which significantly reduced intracellular oxidative stress (OS). However, no significantly improved treatment effect was detected on fat accumulation in the liver sections. The added cholesterol intake in this study was continued daily by diet and stimulation, suggesting that patients should strictly consume a low-cholesterol diet in clinical therapy to minimize the load on the liver. This study demonstrated that the HeShouWu complex reduced blood and liver TC and TG levels satisfactorily. Improvements in the clinical use of the HeShouWu complex are expected to uncover safer, more effective, and economical Chinese herbal formulations for reducing blood lipids.

© 2023 The Authors. Published by Elsevier B.V. on behalf of King Saud University. This is an open access article under the CC BY-NC-ND license (<http://creativecommons.org/licenses/by-nc-nd/4.0/>).

Abbreviations: BW, body weight; GSH-Px, glutathione peroxidase; SOD, superoxide dismutase; CAT, catalase; MDA, malondialdehyde; OS, oxidative stress; TSG, 2,3,5,4'-tetrahydroxy-stilbene-2-O-β-D-glucoside; TG, triglyceride; TC, total cholesterol; AS, atherosclerosis; MAFLD, metabolic dysfunction-associated fatty liver disease; NAFLD, non-alcoholic fatty liver disease; NASH, non-alcoholic steatohepatitis; CVD, cardiovascular disease; CKD, chronic kidney disease; AOAC, Association of Official Analytical Chemists; AACC, American Association for Clinical Chemistry; DPPH, 2,2-diphenyl-1-picrylhydrazyl; HDL-C, high-density lipoprotein cholesterol; LDL-C, low-density lipoprotein cholesterol; GOT, glutamate oxalate transaminase; GPT, glutamate pyruvate transaminase; H&E, hematoxylin and eosin; DTNB, 5, 5'-dithiolbis (2-nitrobenzoic acid); VLDL, very low-density lipoprotein; GSSG, glutathione disulfide; ROS, reactive oxygen species.

* Corresponding author.

E-mail address: pohsien0105@pu.edu.tw (P.-H. Li).¹ These authors contributed equally to this work.

Peer review under responsibility of King Saud University.

<https://doi.org/10.1016/j.arabjc.2023.105280>

1878-5352/© 2023 The Authors. Published by Elsevier B.V. on behalf of King Saud University.

This is an open access article under the CC BY-NC-ND license (<http://creativecommons.org/licenses/by-nc-nd/4.0/>).

1. Introduction

The roots of *Polygonum multiflorum*, commonly known as HeShouWu, have been applied in Chinese medicine based on several centuries of continuous practice as clinical therapy for diseases, such as hyperlipidemia, fatty liver, hyperglycemia, and related disorders while achieving recognizable results (Gu et al., 2020, Li et al., 2020, Lin et al., 2020, Chen et al., 2021, Tekal et al., 2021, Cai et al., 2023). Several studies have been published on HeShouWu, and its primary bioactive components are flavonoids, alkaloids, naphthalenes, anthraquinones (emodin, physcion, and physcion 8-O-β-D-glucopyranoside), stilbene [2,3,5,4'-tetrahydroxy-stilbene-2-O-β-D-glucoside (TSG)], phospholipids, polysaccharides, and polysaccharides (Gu et al., 2020, Li et al., 2020, Lin et al., 2020, Adnan et al., 2021, He et al., 2021, Hu et al., 2021, Tekal et al., 2021, Cai et al., 2023). HeShouWu reportedly reduces triglyceride (TG) and total cholesterol (TC) levels in high-fat diet-induced hyperlipidemia while showing promising outcomes in hyperlipidemia models (lack of Apo E gene and Triton-induced) (Wang et al., 2014, Jung et al., 2020, Li et al., 2020, Lin et al., 2020, Choi and Lee 2021, He et al., 2021).

The role of inflammation in metabolic diseases has been demonstrated. Lipid metabolic disorders increase the risk of diseases, such as atherosclerosis (AS), metabolic dysfunction-associated fatty liver disease [MAFLD, the former name was non-alcoholic fatty liver disease (NAFLD)], and non-alcoholic steatohepatitis (NASH) (Cheng et al., 2019, Koperska et al., 2022, Wang et al., 2022, Zhang et al., 2023). In addition, the inflammation may also develop into cardiovascular disease (CVD) or chronic kidney disease (CKD) (Eslam et al., 2020, Koperska et al., 2022, Zhang et al., 2023). These patients are accompanied by obesity, diabetes, or metabolic comorbidities (diabetes or hypertension) (Lin et al., 2020). The progression occurs with the accumulation of liver lipids, insulin resistance, chronic hepatitis, liver fibrosis, and liver cirrhosis, ultimately leading to hepatocellular carcinoma and liver failure (prevalent in patients who consume alcohol), which is the most common chronic liver disease (Eslam et al., 2020, Lin et al., 2020, Ye et al., 2020, Koperska et al., 2022). The “multiple-hit” theory has been widely recognized as more metabolic evidence is confirmed, which involves oxidative stress (OS), mitochondrial dysfunction, inflammation, endoplasmic reticulum stress, gut microbiota dysbiosis, innate immune disorder, and epigenetics, apart from the causes mentioned above (Wang et al., 2014, Eslam et al., 2020, He et al., 2021, Hu et al., 2021, Zhou et al., 2021, Koperska et al., 2022, Zhu et al., 2022, Fang et al., 2023, Koc et al., 2023).

However, the commonly prescribed drugs (such as simvastatin, metformin, and thiazolidinediones) cause side effects. Hence, it is necessary to develop safe and effective drugs to treat MAFLD (Ji et al., 2019, Liu et al., 2019, Chen et al., 2021, Zahid et al., 2021, Zhou et al., 2021, Koperska et al., 2022, Fang et al., 2023). Several natural bioactive compounds have been proposed to treat MAFLD (Cheng et al., 2019, Gao et al., 2020, Jung et al., 2020, Wang et al., 2020). Their pharmacological effects are protective of hepatic OS and reduce fat accumulation in the liver (Xu et al., 2019, Koperska et al., 2022) while removing lipids from the blood (Nie et al., 2016, Singh and Sashidhara 2017, Cheng et al., 2019, Zahid et al., 2021, Fang et al., 2023). Hence, we conducted a 10-week therapeutic trial of single and complex formulations (which have been used clinically) of HeShouWu in the diet-induced hypercholesterolemia (hyperlipidemia) hamster model. This study evaluated the effects of this decoction on cholesterol and lipid levels in the hamsters, which will help inform clinical use.

2. Materials and methods

2.1. Materials

HeShouWu and its complex formula powder (including *Polygonatum sibiricum* Delar. ex Redoute, dried tangerine peel, turmeric, kudzu root, hawthorn, cassia seeds, and malt) were purchased from Ko-Da Pharmaceutical Co., Ltd. (Taoyuan City, Taiwan). All chemical reagents were purchased directly from Sigma-Aldrich®/Millipore® (Merck KGaA, Darmstadt, Germany) and prepared for use without any further purification.

2.2. Experimental animals

Sixty male, 5-week-old Syrian hamsters were purchased from the National Laboratory Animal Center (Taipei, Taiwan). This animal protocol was approved by the Animal Research Committee of the University of Providence (code 20160607-A05). All operating procedures followed the committee for the control and supervision of animal experiments and the National Institutes of Health Guide for the care and use of laboratory animals. Following a 3-day acclimation period, the animals were grouped ($n = 10$) for the 10-week treatment. All animals were housed under specific pathogen-free conditions, including a constant temperature of $23 \text{ }^{\circ}\text{C} \pm 2 \text{ }^{\circ}\text{C}$, 60–80% humidity, and a 12 h light: 12 h dark cycle (07:00–19:00) (Chou et al., 2022). The diet and drinking water were supplied *ad libitum* during the experiment with daily morning changes. Hamster BW and the diet (collected as dropped feed to be calculated as intake) were recorded daily. The feces were collected immediately and stored sealed at $-20 \text{ }^{\circ}\text{C}$ until analysis. The following equations were used to calculate daily weight gain (g/day) and feed efficiency.

$$\text{Daily gain weight (g/day)} = \text{Final BW} - \text{Initial BW} / \text{Days}$$

$$\text{Feed efficiency} = \text{Daily gain weight} / \text{Food intake}$$

2.3. Sample preparation

Based on the clinical experience of a recommended daily HeShouWu dose of 12–15 g/60 kg BW/day, the dose was set at 14 g/60 kg BW/day for this study. Several studies have reported that the usual Chinese Pharmacopoeia clinical dose is 6–12 g/kg BW/day (Liu et al., 2019, Gu et al., 2020, Xue et al., 2020). The dosage for hamsters was converted to 175 mg/day per 100 g BW. Therefore, as defined in this study, 3% and 6% HeShouWu or its complex formula powder were added to the animal diet in the low- and high-dose groups. The positive control group was on a regular diet, and the negative control group was on a diet with an extra addition of 0.5% cholesterol, while the dietary details of each group and the preparation process (twice/week) are shown in Table 1.

2.4. Physicochemical and bioactive properties evaluation of HeShouWu and its complex formula powder

2.4.1. Basic compositional analysis

The basic composition of HeShouWu and its complex formula powder (including moisture, crude fat, crude protein, crude fiber, and ash) were determined following an Association of Official Analytical Chemists (AOAC) procedure and the American Association for Clinical Chemistry (AACC) protocols described by Huang et al. (Huang et al., 2022).

Table 1
Composition of the daily diet for each group (serving size was 12.8 g per hamster).

Components (%)	Group					
	Positive control	Negative control	Complex formula		HeShouWu	
			Low dose	High dose	Low dose	High dose
Corn starch (α -starch)	53.948	53.448	50.448	47.448	50.448	47.448
Sucrose	10.000					
Casein	19.000					
L-cystine	0.300					
Cellulose	5.000					
Soybean oil	7.000					
TBHQ	0.002					
Cholesterol	–	0.500				
Choline bitartrate [#]	0.250					
Mineral mixture	3.500					
Vitamin mixture	1.000					
HeShouWu	–				3.000	6.000
Complex formula	–		3.000	6.000	–	
Total diet weight	100.000					
Drinking Water	200.000					

[#]Choline bitartrate is a critical component that promotes the availability of cholesterol.

All power to prepare the dietary formulas was added to the mixing tank according to weight and mixed uniformly at a low speed for 15–20 min, followed by slowly adding drinking water (with 10% sucrose) and oil (0.002% TBHQ) several times and mixing to form the dough. Next, the food was divided into pellets (approximately 12.8 g per serving) and stored at $-20\text{ }^{\circ}\text{C}$ until use. Notably, the weight of the sample and 0.5% cholesterol were subtracted from the corn starch. In addition, TBHQ was used as an antioxidant in the formulations to avoid oil oxidation during storage.

2.4.2. In vitro antioxidant ability

HeShouWu and its complex formula powder were extracted with water and 50% alcohol in two modes; regular extraction ($4\text{ }^{\circ}\text{C}$, 1 h) and simulated herbal medicinal decoction extraction ($90\text{ }^{\circ}\text{C}$ for 40 min with shaking at 100 rpm). All extracts were filtered and stored at $-20\text{ }^{\circ}\text{C}$ until use. All extracts were thawed before analysis and then prepared at different concentrations (0.2%, 0.5%, 0.8%, and 1%).

2.4.2.1. 2,2-diphenyl-1-picrylhydrazyl (DPPH) free radical scavenging activity. DPPH free radical scavenging activity was determined following the protocol described by Li et al., (2020) and Wang et al., (2019) with minor modifications. In brief, the 100 μL sample was mixed with 400 μL of Tris-HCl buffer solution (pH 7.4), followed by a reaction with 250 μM DPPH reagent for 20 min in the dark. The background was prepared in 900 μL of Tris-HCl buffer with 100 μL of sample solution, while the control (0.02% gallic acid) was prepared from 400 μL of Tris-HCl buffer and 100 μL of 95% ethanol. Absorbance was determined at 517 nm using a spectrophotometer (Model 7800 Jasco Global, Tokyo, Japan) (baseline with 95% ethanol used for zeroing), and DPPH free radical scavenging activity was calculated using the following formula.

$$\text{DPPH free radical scavenging ability (\%)} = [1 - (\text{OD}_{517_{\text{sample}}} - \text{OD}_{517_{\text{background}}}) / \text{OD}_{517_{\text{control}}}] \times 100$$

2.4.2.2. Reducing power. Reducing power was measured using the method described by Huang et al., (2011) and Liu et al., (2023) with appropriate modifications. The reaction solution consisted of 0.2 M sodium phosphate buffer solution (PBS, pH 6.6) and 1% potassium ferricyanide mixture (150 μL each) with various concentrations of the sample solution, followed by 20 min at $50\text{ }^{\circ}\text{C}$ in a water bath and 3 min cooling in an ice bath. Next, 600 μL of deionized water and 150 μL of 10% trichloroacetic acid solution were added and centrifuged ($1000 \times g$, 5 min). The supernatant was reacted with 150 μL of 0.1% ferric chloride for 15 min, and absorbance was measured at 700 nm. The control group was 0.01% gallic acid. The level of reducing power depended on the absorbance value.

2.4.2.3. Ferrous ion chelating ability. The ferrous ion chelating ability of the samples was determined using the methods described by Huang et al., (2011) with some modifications. The sample solution (250 μL), 25 μL of 2 mM FeCl_2 , and 925 μL of PBS (pH 7.4) were mixed. Then, 50 μL of 5 mM ferrozine was added, followed by a 10 min reaction at room temperature, after which the absorbance of the mixture was measured at 562 nm. The control group was 0.08% gallic acid. The chelating capacity of the metal ions was calculated based on the following equation.

$$\text{Metal ion chelating ability (\%)} = (1 - \text{OD}_{562_{\text{sample}}} / \text{OD}_{562_{\text{control}}}) \times 100$$

2.5. Evaluation of lipid metabolism in feces

2.5.1. Neutral steroid content

Neutral steroid content was quantified according to the method described in Xiong et al., (2007), with appropriate modifications. The dried sample (0.1 g) was extracted with 0.5 mL of petroleum ether for 2 h, followed by centrifugation for 20 min ($2000 \times g$, $4\text{ }^{\circ}\text{C}$). Then, 0.1 mL of the supernatant was volatilized by a nitrogen gas stream under a hood until dry. A 1 mL aliquot of Libermann-Burchard reagent (anhydride, sulfuric acid, and the acetic acid ratio were 20:1:10, v/v/v) was added, followed by a colorimetric reaction (showed light green color) for 20 min at room temperature ($25\text{ }^{\circ}\text{C}$). The absorption value was determined at 550 nm, and a standard curve was prepared for the various cholesterol concentrations. Neutral sterol content in the feces was calculated by interpolation.

2.5.2. Total bile acid content

The total bile acid content of the feces was determined following the standard operating procedures provided by the manufacturer of the bile acids (total) assay kit (Randox Laboratories Ltd., Antrim, UK).

2.6. Blood biochemical analysis

The blood biochemical analysis was performed as described by Chou et al., (2022). The blood was collected and centrifuged (10 min, $4\text{ }^{\circ}\text{C}$, $12,000 \times g$) in a microfuge (22R, Beckman Coulter

Inc., Brea, CA, USA) immediately after the hamsters were killed. The plasma biochemical parameters, including TG, TC, high-density lipoprotein cholesterol (HDL-C), low-density lipoprotein cholesterol (LDL-C), glutamate oxalate transaminase (GOT), and glutamate pyruvate transaminase (GPT), were analyzed using the Synchron LX-20 system (Beckman-Coulter).

2.7. Blood, liver, and kidney samples

The hamsters were anesthetized with an intraperitoneal injection of sodium pentobarbital before death; blood was collected from the heart, and the liver and kidneys were excised and rinsed clean with physiological saline (0.9% NaCl solution). Finally, the appearance of the organs was recorded with a digital camera, and the organs were weighed. The largest piece of the liver was cut off, and sampling was performed in the middle, while the other parts were sealed and stored at $-20\text{ }^{\circ}\text{C}$ until further analysis.

2.8. Liver pathology

The pathological sections were prepared according to the protocol described in Brasil et al., (2022) and Dai et al., (2023) with minor modifications. In brief, the liver tissues were fixed in 10% formalin for 24 h. The tissues were dehydrated in absolute alcohol (70%, 80%, 90%, 95%) and cleared in xylene. The fixed tissues were embedded in paraffin, cut into 4 μm thick sections, stained with hematoxylin and eosin (H&E), and photographed with an Olympus fluorescence microscope (U-LH100HG, Olympus Co., Tokyo, Japan). The fatty liver was scored as 0 for no fat observed; 1 for $< 5\%$ of liver tissue surface replaced by fat; 2 for 5–25%; 3 for 25–50% of fat; and 4 for $> 50\%$.

2.9. Liver TG and TC contents

2.9.1. Preparation of the liver extracts

The liver extracts were prepared according to the protocol described by Reiter et al., (2022) with minor modifications. A 0.5 g portion of liver tissue was added to a 20-fold Folch solution (chloroform and methanol ratio of 2:1, v/v), homogenized for 5 min with a homogenizer (PRO250[®], Thomas Scientific., Swedesboro, NJ, USA), filtered, weighed, and quantified with Folch solution to 10 mL.

2.9.2. TG and TC content

The extract (0.3 mL; section 2.9.1) was weighed and concentrated under a stream of nitrogen, then 0.3 mL of 2% Triton X-100 was added; 10 μL was mixed with 1 mL of Libermann-Burchard Reagen at room temperature for 10 min, and the absorbance value was measured at 500 nm. The standard curve was prepared with cholesterol and triglyceride standards, and liver TG and TC contents were calculated by interpolation.

2.10. In vivo antioxidant activity and biochemical analysis of the organs

2.10.1. Preparation of the tissue homogenate

The animal tissue homogenates were prepared according to the protocol of Li et al., (2020) and Simpson (2010), with minor modifications. A tissue homogenized stock of the liver (0.3 g) and whole kidney was prepared, respectively, by adding 0.5 mL of 50 mM PBS (pH 7.4) followed by homogenization (1,400 rpm, 30 sec) in an ice bath. A 40 μL aliquot of each stock was added to 56 μL of PBS and 96 μL of 2% Triton X-100, mixed, and centrifuged at $10,000 \times g$ for 5 min at $4\text{ }^{\circ}\text{C}$; the supernatant was used for analysis. This sample preparation procedure was repeated for each assay below.

2.10.2. GSH-Px activity

GSH-Px activity was measured using a procedure slightly modified from Kong et al. (Kong et al., 2018). The sample (50 μL) was added to 450 μL of 0.25 M potassium phosphate buffer (pH 7.4) (diluted 10-fold). Next, 100 μL of the diluted sample was mixed with 200 μL of GSH reductase (GSSH-R, 5 U/mL), 50 μL of 40 mM GSH, and 620 μL of potassium phosphate buffer solution in that order. Then, 10 μL of 20 mM NADPH (freshly prepared) was added followed by 20 μL of 15 mM cumene hydroperoxide. Absorbance was measured immediately at 340 nm (absorbance values were read every 15 sec at $25\text{ }^{\circ}\text{C}$ to determine the change within 1 min). GSH-Px activity (U) was defined as the number of micromoles per min of NADPH oxidation ($\epsilon_{340} = 6.1\text{ cm}^2/\mu\text{mole}$).

2.10.3. SOD activity

SOD activity was determined as described by Li (2012) and Senthilkumar et al., (2021) with modifications. A 10 μL aliquot of sample was mixed with 3 mL of Tris-HCl buffer (50 mM, pH 8.2), and 15 μL of pyrogallol (50 mM) was added and shaken three times. The absorbance of the solution was measured at 325 nm (every 15 sec to determine the change of absorbance in 1 min). The control group used 10 μL of deionized water.

2.10.4. CAT activity

CAT activity was determined following the protocol described by Aebi (1984), with modifications. The sample (10 μL) was diluted 1,000-fold with 50 mM PBS (pH 7.0), and then 2 mL was mixed with 1 mL of 30 mM H_2O_2 solution. The absorbance was measured at 240 nm (every 15 sec to determine the absorbance change in 1 min). CAT activity (U) was defined as the number of millimoles of H_2O_2 consumed per min. ($\epsilon_{240} = 40\text{ cm}^2/\mu\text{mole}$).

2.10.5. Total protein content

Protein content was determined following the manufacturer's protocol (Thermo Fisher Scientific Inc., Waltham, MA, USA). The sample (10 μL) was diluted 50-fold with 50 mM PBS (pH 7.0), and 500 μL was added to 1 mL of the Pierce[™] BCA protein assay solution, mixed uniformly, and placed in a $37\text{ }^{\circ}\text{C}$ water bath for 30 min. The absorbance was determined at 562 nm after cooling in an ice bath. A standard curve was prepared with bovine serum albumin, and the protein content of the sample was calculated by interpolation.

2.10.6. MDA content

MDA content was measured following the method described by Senthilkumar et al., (2021), with some modifications. A 200 μL aliquot of the sample (serum or tissue homogenate) was homogenized with 75 μL of 0.2% BHT solution and 500 μL of 0.6% TBA solution for 1 min, followed by a $90\text{ }^{\circ}\text{C}$ water bath for 45 min, an ice bath for 15 min, and centrifugation ($1,000 \times g$, $4\text{ }^{\circ}\text{C}$) for 15 min. Next, 700 μL of the supernatant was added to 700 μL of n-butanol, homogenized for 1 min, and then centrifuged ($3,000 \times g$, $4\text{ }^{\circ}\text{C}$) for 15 min. Finally, 600 μL of the supernatant was used to determine the absorbance at 532 nm. A standard curve was prepared using TEP (1, 1, 3, 3-tetra ethoxy propane), and the MDA content of the sample was calculated by interpolation.

2.10.7. Total thiol content

Total thiol content was determined as described by Aitken and Learmonth (2009) with minor modifications. After diluting the sample 1,000-fold, 25 μL was added to 750 μL of PBS (pH 7.4) and 50 μL of 5, 5'-dithiolbis (2-nitro-benzoic acid) (DTNB) was reacted for 3 min. Absorbance was determined at 412 nm. Finally, total thiol content of the sample was calculated using the formula:

$$\text{Total thiol } (\mu\text{mol/g tissue}) = \text{OD}_{412\text{Sample}} / 14150 \times 1 \times 33 \times 10^3 \times 1000$$

Where 14,150 means that the extinction coefficient of DTNB is $14150 \text{ M}^{-1}\text{cm}^{-1}$, and 1,000 is the dilution ratio.

2.11. Statistical analysis

Statistical analysis was performed using SAS statistical software (version 9.1, SAS Institute, Cary, NC, USA). The results are expressed as mean \pm SEM. All data were analyzed by one-way analysis of variance and Duncan's new multiple-range test to detect differences between the groups. A p -value of < 0.05 was considered significant.

3. Results and discussion

3.1. Basic composition and bioactivity of the Chinese herb samples

The basic composition of HeShouWu and its complex formula were analyzed as moisture, crude fat, crude protein, crude fiber,

Table 2

The basic composition of HeShouWu (*Polygonum multiflorum*) and its complex formula.

Basic composition (%)	Complex formula	HeShouWu
Moisture	7.71 \pm 0.06 ^b	12.25 \pm 0.02 ^a
Crude fat	2.02 \pm 0.12 ^b	7.14 \pm 0.13 ^a
Crude protein	4.73 \pm 0.09 ^a	1.42 \pm 0.02 ^b
Crude fiber	72.56 \pm 0.85 ^a	61.16 \pm 0.38 ^b
Ash	4.40 \pm 0.06 ^a	4.32 \pm 0.07 ^a

Means with different letters in the same column are significantly different ($p < 0.05$).

All data are expressed as the dried base.

Table 3

Effect of different extracts on antioxidant capacity (DPPH free radical scavenging ability, reducing power, and ferrous ion chelating ability) of HeShouWu (*Polygonum multiflorum*) and its complex formula.

Antioxidation ability	Group	Conc. (%)	Cold		Hot			
			Water	Alcohol	Water	Alcohol		
DPPH free radical scavenging ability (%)	Complex formula	0.2	33.5 \pm 0.3 ^a	29.3 \pm 0.1 ^b	25.2 \pm 0.3 ^d	25.8 \pm 0.0 ^c		
		0.5	65.2 \pm 0.6 ^a	58.8 \pm 0.2 ^b	51.4 \pm 0.7 ^c	58.6 \pm 1.2 ^b		
		0.8	81.6 \pm 0.1 ^a	71.3 \pm 0.0 ^c	70.5 \pm 0.7 ^d	76.1 \pm 0.3 ^b		
		1.0	82.8 \pm 0.2 ^b	79.9 \pm 0.2 ^c	83.5 \pm 0.0 ^a	83.6 \pm 0.2 ^a		
		0.2	16.5 \pm 0.2 ^c	17.2 \pm 0.4 ^b	18.2 \pm 0.7 ^a	15.6 \pm 0.4 ^d		
	HeShouWu	0.5	42.0 \pm 0.2 ^a	32.4 \pm 0.0 ^c	37.2 \pm 0.0 ^b	30.3 \pm 0.4 ^d		
		0.8	52.7 \pm 0.7 ^b	40.0 \pm 0.4 ^d	61.7 \pm 1.3 ^a	46.2 \pm 1.3 ^c		
		1.0	60.7 \pm 0.2 ^b	47.9 \pm 0.1 ^d	73.5 \pm 0.0 ^a	59.7 \pm 0.3 ^c		
		Reducing power	Complex formula	0.2	0.55 \pm 0.01 ^a	0.50 \pm 0.00 ^a	0.41 \pm 0.02 ^b	0.48 \pm 0.03 ^a
				0.5	1.11 \pm 0.02 ^a	1.05 \pm 0.04 ^{ab}	0.76 \pm 0.02 ^c	0.99 \pm 0.01 ^b
0.8	1.61 \pm 0.01 ^a			1.32 \pm 0.14 ^b	0.99 \pm 0.01 ^c	1.57 \pm 0.02 ^a		
1.0	2.52 \pm 0.04 ^a			1.75 \pm 0.10 ^c	1.39 \pm 0.02 ^d	1.97 \pm 0.01 ^b		
HeShouWu	0.2		0.40 \pm 0.00 ^a	0.34 \pm 0.00 ^b	0.34 \pm 0.00 ^b	0.32 \pm 0.00 ^b		
Ferrous ion chelating ability (%)	Complex formula	0.5	0.80 \pm 0.02 ^a	0.67 \pm 0.02 ^b	0.70 \pm 0.00 ^b	0.60 \pm 0.00 ^c		
		0.8	1.05 \pm 0.01 ^a	0.83 \pm 0.02 ^c	0.96 \pm 0.01 ^b	0.84 \pm 0.01 ^c		
		1.0	1.43 \pm 0.07 ^a	1.07 \pm 0.09 ^{bc}	1.19 \pm 0.02 ^b	0.98 \pm 0.02 ^c		
		0.2	26.8 \pm 0.9 ^a	25.9 \pm 1.9 ^a	7.6 \pm 1.9 ^c	19.6 \pm 3.0 ^b		
		0.5	42.5 \pm 2.6 ^b	48.5 \pm 3.0 ^a	21.1 \pm 2.5 ^d	36.5 \pm 2.8 ^c		
	0.8	59.5 \pm 3.1 ^b	64.0 \pm 1.5 ^a	30.0 \pm 3.2 ^c	58.5 \pm 2.5 ^b			
HeShouWu	1.0	65.9 \pm 5.1 ^a	71.6 \pm 0.4 ^a	40.3 \pm 2.7 ^b	66.5 \pm 1.1 ^a			
0.2	7.4 \pm 0.9 ^d	22.4 \pm 1.1 ^a	10.0 \pm 1.2 ^c	19.3 \pm 0.6 ^b				
0.5	32.4 \pm 1.8 ^c	37.7 \pm 0.8 ^b	20.5 \pm 0.6 ^d	40.0 \pm 0.6 ^a				
0.8	53.9 \pm 4.1 ^c	61.3 \pm 1.9 ^b	61.3 \pm 1.9 ^b	65.8 \pm 2.1 ^a				
1.0	52.7 \pm 8.2 ^c	70.5 \pm 1.3 ^b	41.5 \pm 0.5 ^d	76.6 \pm 4.8 ^a				

Conc.: Concentration.

Means with different letters in the same column are significantly different ($p < 0.05$).

and ash contents. The results showed that there were significant differences ($p < 0.05$) between the two formulations in terms of moisture, crude fat, crude protein, and crude fiber (Table 2). Chinese herbs are traditionally consumed by decoction or extracted in hot water or alcohol (Liu et al., 2019, Choi and Lee 2021). Therefore, in this study, two extraction modes were used, and different concentrations of the extracts were used to evaluate the antioxidant capacity of the Chinese herbs. DPPH radical scavenging activity was dose-dependent among the groups, in which the complex group had significantly higher DPPH radical scavenging activity than the HeShouWu group ($p < 0.05$) (Table 3). Moreover, the DPPH radical scavenging activities of the complex groups extracted with cold water, cold alcohol, and hot alcohol were significantly higher than that of the hot water extract ($p < 0.05$) (Table 3). This result suggests that the extract may contain other components (such as emodin, rhein, chrysophanol, resveratrol, and aloe-emodin) besides total phenolic compounds, which provide hydrogen ions to promote the DPPH radical scavenging effect (Xue et al., 2020). Notably, viable keto-enol conversion with facilitated production of hydrogen ions for free radical scavenging effects is present in these quinone compounds (Paul et al., 2020). The results for reducing power were also dose-dependent, with significant differences among all groups ($p < 0.05$), and the complex formula had significantly higher reducing power than HeShouWu ($p < 0.05$) (Table 3). We hypothesized that the combination of the alcoholic decoction did not facilitate an increase in reducing power. Moreover, ferrous ion chelating ability was also dose-dependent among the groups, particularly in the case of hot water and hot alcohol extracts, and the ferrous ion chelating ability of the complex formula was significantly higher than that of HeShouWu ($p < 0.05$) (Table 3). However, the cold and hot extracts had similar DPPH radical scavenging ability and reducing power. Thus, the traditional decoction with hot water continues to be used for preparing samples in animal studies, which also meets the practical requirements for clinical application (Chen et al., 2021, Choi and Lee 2021).

3.2. Evaluation of growth performance in the experimental animals

The group average daily intake results were not significantly different, albeit with slight differences (Table 4). In particular, the food intake of the high-dose HeShouWu group was significantly higher than that of the control ($p < 0.05$). However, this indicated that the diets supplemented cholesterol and HeShouWu did not disturb the daily feeding of the hamsters. Moreover, taking into account the results of final body weight, daily gain weight, and feed efficiency together, the following might be hypothesized while the HeShouWu complex may have the potential benefits for BW loss. In contrast, HeShouWu may have an appetite-suppressing ability.

The BWs of the low-dose and high-dose HeShouWu groups were significantly different ($p < 0.05$) compared with the other groups (Table 4). However, the final BW was not significantly different. The low-dose and high-dose HeShouWu groups revealed significantly lower daily weight gain than the other groups ($p < 0.05$) (Table 4). The same results were obtained regarding feed efficiency ($p < 0.05$) (Table 4). These results suggest that the low- and high-doses of HeShouWu may have inhibited the metabolism of hamsters, which agreed with the findings of Choi and Lee (2021). In contrast, no significant difference was observed between the added cholesterol and the HeShouWu complex groups compared with the positive control group, indicating that the growth and

metabolism of hamsters were unaffected. Moreover, a 70% ethanol extract of HeShouWu fractions (emodin, chrysophanol, emodin-8-O- β -D-glucopyranoside, (cis)-emodin-emodin dianthrones, and (trans)-emodin-emodin dianthrones) were hepatotoxic and inhibited growth of zebrafish (*Danio rerio*). Notably, it has been confirmed in a genetic knockout (CYP3A4 or UGT1A1) liver and liver stem cell model that TSG, the primary active substance in HeShouWu, is not hepatocytotoxic (Hu et al., 2021). Taken together, these findings suggest that the hepatotoxicity of HeShouWu should be regulated during cultivation, preparation, and formulation (dosage and time) (Liu et al., 2019; Chen et al., 2021; Choi and Lee 2021, Hu et al., 2021, Teka et al., 2021, Zahid et al., 2021, Wang et al., 2022). Simultaneously, the patient's uniqueness (healthy constitution and disease profile) should also be considered (Xue et al., 2020, Teka et al., 2021). In addition, about 40% of patients with MAFLD are not obese (Ye et al., 2020). Although obesity is a crucial determinant of MAFLD, as shown by epidemiological data, it should not be the primary marker for screening (Koperska et al., 2022).

3.3. Neutral sterol and total bile acid content in feces

The development of steatosis partly depends on consuming a high-fat diet, while cholesterol and TG levels rise and activate OS (Drescher et al., 2019). Moreover, cholesterol in the blood of mam-

Table 4

Evaluation of growth performance, lipid content in feces and serum, transaminase activity (GOT and GTP), liver (weight, sections status, and lipids contents), and antioxidant capacity *in vivo* (organs and serum) of hamsters fed with HeShouWu (*Polygonum multiflorum*) and its complex formula, positive and negative control groups.

Items	Group*						
	Control		Complex formula		HeShouWu		
	Positive	Negative	Dose		Low	High	
			Low	High	Low	High	
Growth and diet							
Intake (g/day)	10.15 \pm 0.63 ^b	10.43 \pm 0.43 ^b	10.16 \pm 0.55 ^b	10.61 \pm 0.56 ^{ab}	10.63 \pm 0.46 ^{ab}	10.94 \pm 0.24 ^a	
Initial weight (g)	72.90 \pm 4.99 ^b	72.97 \pm 3.58 ^b	75.62 \pm 4.76 ^b	76.67 \pm 3.80 ^{ab}	81.07 \pm 7.33 ^a	80.71 \pm 5.22 ^a	
Final weight (g)	116.10 \pm 9.70 ^a	111.88 \pm 10.57 ^a	112.35 \pm 7.80 ^a	112.25 \pm 5.70 ^a	115.21 \pm 8.24 ^a	114.18 \pm 6.44 ^a	
Daily gain weight (g/day)	0.59 \pm 0.10 ^a	0.58 \pm 0.09 ^a	0.54 \pm 0.07 ^{ab}	0.55 \pm 0.06 ^{ab}	0.49 \pm 0.05 ^b	0.49 \pm 0.05 ^b	
Feed efficiency	0.058 \pm 0.009 ^a	0.055 \pm 0.008 ^a	0.053 \pm 0.007 ^a	0.052 \pm 0.006 ^{ab}	0.046 \pm 0.005 ^b	0.045 \pm 0.005 ^b	
Feces lipids							
Sterol in feces (mg/g feces)	3.65 \pm 0.04 ^c	21.14 \pm 1.53 ^b	24.62 \pm 1.67 ^a	21.79 \pm 1.14 ^b	22.05 \pm 1.06 ^b	23.84 \pm 1.23 ^a	
Total bile acid in feces (μ g/g feces)	200.70 \pm 18.10 ^c	440.40 \pm 17.60 ^b	451.50 \pm 30.80 ^{ab}	485.40 \pm 40.50 ^a	435.70 \pm 32.70 ^b	429.00 \pm 38.70 ^b	
Serum lipids (mg/dL)							
Triglycerides (TG)	53.43 \pm 11.00 ^b	82.88 \pm 27.43 ^a	57.08 \pm 6.89 ^b	54.34 \pm 7.26 ^b	54.34 \pm 7.26 ^b	68.36 \pm 6.66 ^b	
Total cholesterol (TC)	76.40 \pm 11.53 ^d	238.13 \pm 17.86 ^a	195.65 \pm 23.78 ^b	195.21 \pm 18.48 ^b	171.90 \pm 15.43 ^c	209.96 \pm 33.03 ^b	
High-density lipoprotein cholesterol (HDL-C)	31.60 \pm 4.85 ^c	75.02 \pm 9.39 ^{ab}	73.92 \pm 7.46 ^{ab}	78.33 \pm 7.70 ^a	67.53 \pm 6.52 ^b	81.33 \pm 10.78 ^a	
Low-density lipoprotein cholesterol (LDL-C)	51.07 \pm 9.72 ^d	156.23 \pm 11.43 ^a	134.58 \pm 16.80 ^b	122.30 \pm 19.44 ^{bc}	114.13 \pm 8.13 ^c	133.51 \pm 30.13 ^b	
HDL-C/LDL-C ratio	0.75 \pm 0.06 ^a	0.53 \pm 0.12 ^b	0.59 \pm 0.16 ^b	0.62 \pm 0.08 ^b	0.59 \pm 0.08 ^b	0.63 \pm 0.10 ^b	
Serum transaminase activity (U/dL)							
Glutamate oxalate transaminase (GOT)	15.47 \pm 0.86 ^c	50.46 \pm 4.92 ^b	50.61 \pm 5.99 ^b	65.53 \pm 4.05 ^a	54.26 \pm 4.36 ^b	62.83 \pm 6.26 ^a	
Glutamate pyruvate transaminase (GPT)	16.66 \pm 0.71 ^c	33.64 \pm 3.42 ^{ab}	28.16 \pm 6.31 ^b	36.57 \pm 1.10 ^a	14.76 \pm 0.95 ^c	32.45 \pm 1.79 ^{ab}	
Liver lipids							
Wet weight (g) per 100 g body weight	2.80 \pm 0.10 ^b	5.50 \pm 0.30 ^a	5.50 \pm 0.20 ^a	5.30 \pm 0.50 ^a	5.30 \pm 0.20 ^a	5.50 \pm 0.20 ^a	
Fatty liver score	0.00 \pm 0.00 ^b	3.20 \pm 0.40 ^a	3.30 \pm 0.50 ^a	3.50 \pm 0.50 ^a	3.20 \pm 0.40 ^a	3.30 \pm 0.50 ^a	
Triglycerides (TG) (mg/dL)	1.50 \pm 0.20 ^e	39.50 \pm 2.40 ^a	22.30 \pm 7.60 ^b	19.80 \pm 2.60 ^{bc}	16.70 \pm 2.60 ^{cd}	13.60 \pm 2.70 ^d	
Total cholesterol (TC) (mg/dL)	11.60 \pm 1.00 ^c	29.30 \pm 7.70 ^a	17.70 \pm 2.90 ^b	15.50 \pm 1.60 ^b	16.90 \pm 1.20 ^b	18.10 \pm 1.90 ^b	
Antioxidant activity of organs and serum (μmol/g tissue)							
Malondialdehyde (MDA)	Liver	0.050 \pm 0.001 ^c	0.085 \pm 0.002 ^a	0.019 \pm 0.003 ^f	0.028 \pm 0.001 ^d	0.070 \pm 0.001 ^b	0.023 \pm 0.003 ^e
	Kidney	0.46 \pm 0.01 ^{bc}	0.61 \pm 0.03 ^a	0.44 \pm 0.02 ^c	0.43 \pm 0.01 ^c	0.48 \pm 0.02 ^b	0.48 \pm 0.01 ^b
	Serum	0.010 \pm 0.001 ^b	0.014 \pm 0.001 ^a	0.010 \pm 0.001 ^b	0.005 \pm 0.001 ^d	0.006 \pm 0.001 ^{dc}	0.006 \pm 0.001 ^c
Total thiol	Liver	1.26 \pm 0.01 ^e	2.51 \pm 0.07 ^c	2.07 \pm 0.02 ^d	2.07 \pm 0.03 ^d	3.04 \pm 0.02 ^a	2.72 \pm 0.06 ^b
	Kidney	3.76 \pm 0.06 ^e	5.57 \pm 0.14 ^c	6.09 \pm 0.07 ^a	5.81 \pm 0.03 ^b	5.42 \pm 0.04 ^d	5.91 \pm 0.07 ^b

*n = 10.

Means with different letters in the same row are significantly different ($p < 0.05$).

mals is derived from biosynthesis in the liver and peripheral tissues or absorption of cholesterol by the intestines (Akbulut et al., 2022). Both ways are critical for maintaining hepatic cholesterol stores and the homeostatic balance of cholesterol metabolism. Cholesterol clears 1%–2% of the bile salts in fecal microaggregates. However, about 98% of the bile re-enters the liver via the classic enterohepatic circulation of bile acids and is absorbed by the ileum.

Fecal-neutral sterols were the highest in the low-dose complex group (24.62 mg/g feces), followed by the high-dose HeShouWu group (23.84 mg/g feces), which were significantly different from the positive and negative control groups ($p < 0.05$) (Table 4). These results suggest that low-dose complex and high-dose HeShouWu promoted cholesterol metabolism with a higher level of neutral sterols in the feces. However, the low-dose HeShouWu and high-dose complex groups were not significantly different from the negative control group. A significant increase in fecal-neutral sterols was associated with excess dietary cholesterol intake.

The highest total bile acid content in feces was detected in the high-dose complex group (485.4 $\mu\text{L}/\text{mg}$), compared with the other groups ($p < 0.05$) (Table 4). Total bile acid content in feces of the low-dose complex group (451.5 $\mu\text{L}/\text{mg}$) was slightly higher than the negative control group (440.4 $\mu\text{L}/\text{mg}$) (Table 4). These results suggest that high dietary cholesterol intake supplemented with the HeShouWu complex significantly contributed to the metabolism of total bile acids (Xue et al., 2020). Notably, the homeostatic balance of cholesterol metabolism (synthesis, absorption, and clearance) in the body affects the cholesterol level in the blood.

3.4. Blood biochemical analysis

3.4.1. Serum lipids

Cholesterol in the blood is typically transported to the liver via HDL-C for absorption, storage, and metabolism, contributing to lower cholesterol levels in the blood and potentially reducing the risk of AS (Ji et al., 2019, Liu et al., 2019, Jung et al., 2020, Akbulut et al., 2022). The negative control group had significantly higher levels of all indicators ($p < 0.05$) than the treated groups (Table 4). In particular, there was a 2.4-fold gap ($p < 0.05$) in the blood TC levels between the positive (53.43 mg/dL) and negative (82.88 mg/dL) control groups, which was attributed to the high-cholesterol diet, which contributed to increase HDL-C and LDL-C levels. However, the blood TG of the four groups treated with HeShouWu and its complex was significantly different from the negative control group (238.13 mg/dL) ($p < 0.05$). Only the low-dose HeShouWu (171.90 mg/dL), low-dose (195.65 mg/dL), and high-dose (195.21 mg/dL) complex groups had significantly different TC levels from the negative control group (238.13 mg/dL) ($p < 0.05$), suggesting that low-dose HeShouWu and its complex effectively reduced blood TG and TC (Table 4). In addition, no significant difference in the HDL-C level was observed among the four groups supplemented with HeShouWu or its complex (67.53–81.33 mg/dL) compared to the negative control group (75.02 mg/dL). In contrast, LDL-C levels were significantly different among these groups ($p < 0.05$). In particular, the low-dose HeShouWu (114.13 mg/dL) and high-dose HeShouWu complex (122.3 mg/dL) groups lowered LDL-C levels (Table 4). Wang et al., (2014) reported that TSG from HeShouWu and its extract inhibits cholesterol synthase and increases the expression of the LDL receptor to catabolize serum cholesterol (LDL receptor pathway). Moreover, liver LDL receptors affect the rate of LDL synthesis and very low-density lipoprotein (VLDL) metabolism. The indicator that affects AS is the HDL-C/LDL-C ratio; a high value indicates that HDL-C is higher and LDL is lower, which also means that blood TC is more vulnerable to transport to the liver, thereby facilitating a reduced risk of AS (Ji et al., 2019, Zahid et al., 2021, Wang et al., 2022). In

contrast, a low HDL-C/LDL-C ratio means that LDL is higher (and HDL is lower), and the risk of AS increases. However, in this study, the HDL-C/LDL-C ratio of the four therapy groups was slightly higher than that in the negative control group (0.53 ± 0.12 ; $p > 0.05$). Nevertheless, the HDL-C/LDL-C ratio of the high-dose HeShouWu (0.63 ± 0.10) and high-dose complex (0.62 ± 0.08) groups remained high and closer to the value of the positive control group (0.75 ± 0.06) ($p < 0.05$) (Table 4). Hence, HeShouWu and its complex slightly mitigated the risk of AS (Jung et al., 2020, Li et al., 2020, Xue et al., 2020).

3.4.2. Serum GOT/GPT

GOT and GPT are important enzymes that participate in synthesizing amino acids and are significant indicators of liver function, generally at concentrations < 40 U/L. However, inflammation or cell damage, such as acute/chronic viral hepatitis, alcoholic liver disease, fatty liver, drug-induced hepatitis, hepatocellular carcinoma, cirrhosis, or intra- and extra-hepatic cholestasis, all contribute to increasing the serum levels of GOT and GPT (Jung et al., 2020, Zhang et al., 2023). Specifically, increases in GOT and GPT indicate liver inflammation (Wang et al., 2020). The increases in GOT are more pronounced than those of GPT in cases of AS, myocardial infarction, or alcoholic hepatitis.

In this study, all groups were significantly different from the control group ($p < 0.05$) (Table 4); GOT was higher than GPT, suggesting that a high intake of cholesterol caused signs of liver inflammation. However, the high-dose HeShouWu (62.83 U/dL) and the complex (65.53 U/dL) groups exhibited significantly higher GOT levels than the other groups ($p < 0.05$) (Table 4). Unfortunately, this result suggests that other substances promoted inflammation in the high-dose group. However, the phenomenon of such increasing is not well understood, and metabolomics' impact requires further investigation. This was not observed in the low-dose HeShouWu (54.26 U/dL) or complex (50.61 U/dL) groups, which had a similar GOT level as that in the negative control group (50.46 U/dL) ($p < 0.05$) (Table 4). The bioactive components of HeShouWu have been reported to remove O_2^- , OH^- , and H_2O_2 radicals, which leads to lower levels of GPT and GOT (Xue et al., 2020). Notably, the GPT results were similar in the high-dose HeShouWu group (32.45 U/dL) and the complex (36.57 U/dL) compared to the negative control group (33.64 U/dL) ($p < 0.05$) (Table 4), and previous findings were consistent with those reported here.

3.5. Evaluation of liver pathology

AS, NASH and MAFLD are characterized by fat deposits in liver cells, leading to a fatty liver, which subsequently develops into chronic inflammation (Drescher et al., 2019, Li et al., 2020). Prolonged inflammation leads to fibrosis and cirrhosis, associated with obesity and metabolic diseases (hyperlipidemia and type II diabetes) (Nie et al., 2016, Eslam et al., 2020, Lin et al., 2020). The purple spots on the H&E-stained liver pathological sections are cell nuclei, the pink dots are red blood cells, and the pink areas are hepatocytes (Fig. 1). The pathological sections clearly showed a significant difference between the positive control group and the treatment groups, and a significant difference in the scores was observed ($p < 0.05$) (Table 4). In particular, the negative control group accumulated significantly more fatty particles among hepatocytes, resulting in a score of 3.2 ± 0.4 . No significant difference in liver fat accumulation or score (3.2–3.3) was detected in the four therapy groups compared with the negative control group, suggesting that HeShouWu and its complex did not improve fat accumulation in the MAFLD liver. However, Gu et al., (2020) reported that HeShouWu alleviates hepatocyte steatosis, particularly at a high dose (1.62 g/kg BW). The discrepancy was attributed to differ-

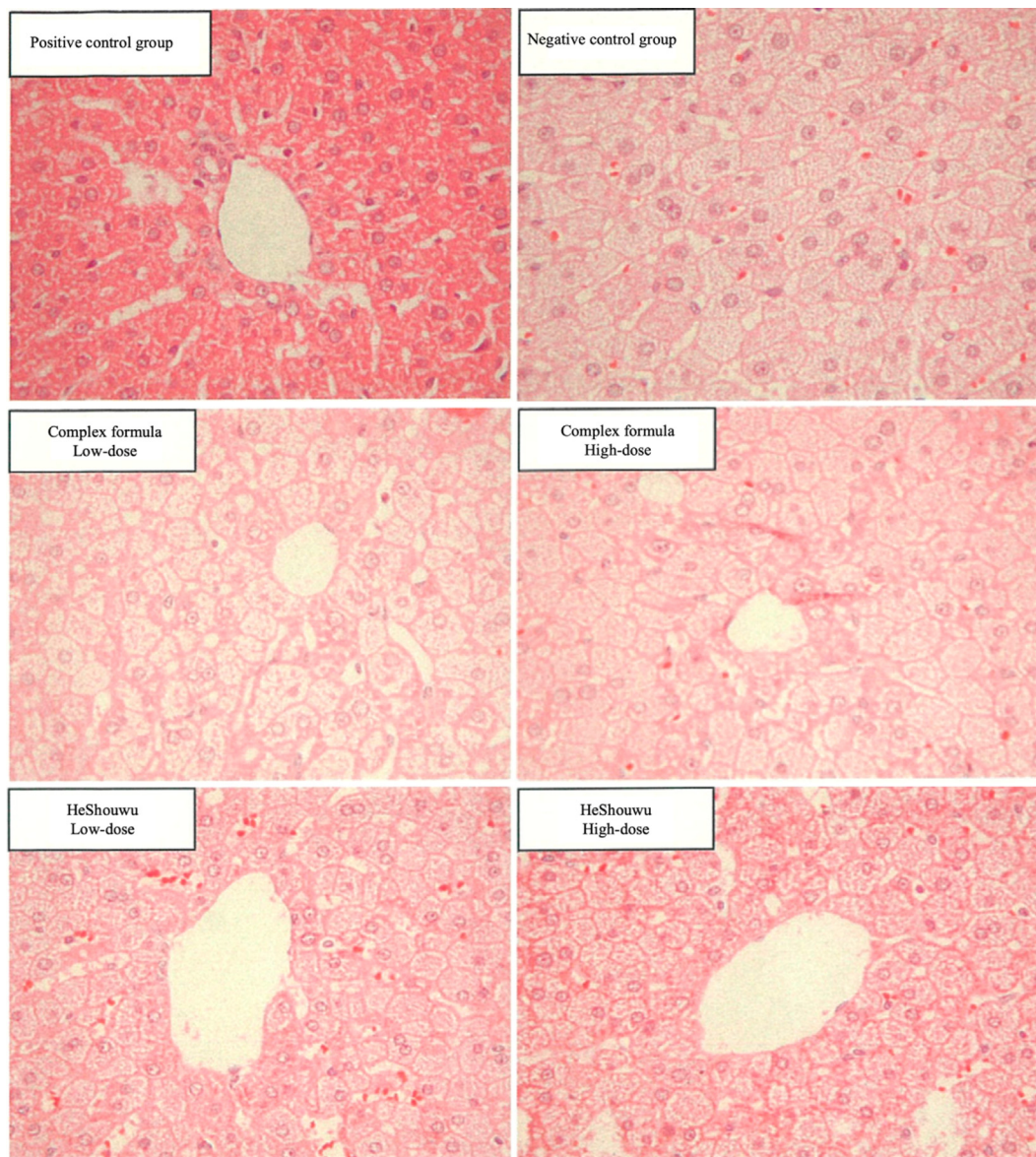


Fig. 1. Histopathological section of hamsters fed with HeShouWu (*Polygonum multiflorum*) and its complex formula, positive and negative control groups hamsters' liver (Magnification ratio $400\times$).

ences in the animal species, diet composition, sample preparation (decoction), and the location of origin, which led to variations in results and available active components (Jung et al., 2020, Chen et al., 2021, Choi and Lee 2021).

3.6. Weight, and liver TC and TG contents

Liver weight was significantly different ($p < 0.05$) between the positive control group (2.8 g/100 g BW) and the others (Table 4). The negative control group (5.5 g/100 g BW) did not differ from the four treatment groups (5.3–5.5 g/100 g BW).

Liver TC and TG contents were significantly different ($p < 0.05$) between the four treatment groups and the negative control group (Table 4), indicating that HeShouWu and its complex reduced liver TC and TG contents (Xu et al., 2019, Jung et al., 2020). In particular, the high dose of HeShouWu reduced TC (13.6 mg/dL) the most, while the high dose of the HeShouWu complex reduced TG (15.5 mg/dL) the most. Gu et al., (2020) reported lower serum LDL-C and a higher HDL-C after HeShouWu treatment, which reduced the accumulation of TG in the liver and was similar to

the results in this study. Moreover, TG and TC were significantly higher in the negative control group, confirming that the MAFLD model with a cholesterol-supplemented diet caused the accumulation of TC and TG in the livers of the hamsters. Taken together, these results suggest that HeShouWu and its complex prevented increases in TC and TG in high-cholesterol diet-fed hamsters (Xue et al., 2020).

3.7. In vivo antioxidant activities

All cells contain the non-enzymatic antioxidant GSH protected from OS by its oxidized form glutathione disulfide (GSSG), which maintains cellular redox homeostasis by acting as a cofactor for several detoxifying enzymes (GPx and GST) (Valko et al., 2006, Barakat et al., 2022). The high and low doses of the HeShouWu complex resulted in significantly exhibiting higher liver GSH-Px activity than in the other groups ($p < 0.05$) (Fig. 2A1). This result indicates that the HeShouWu complex enhanced GSH-Px activity in the liver. GSH-Px activity was higher in the kidney in response to the high and low doses of HeShouWu, with significant differ-

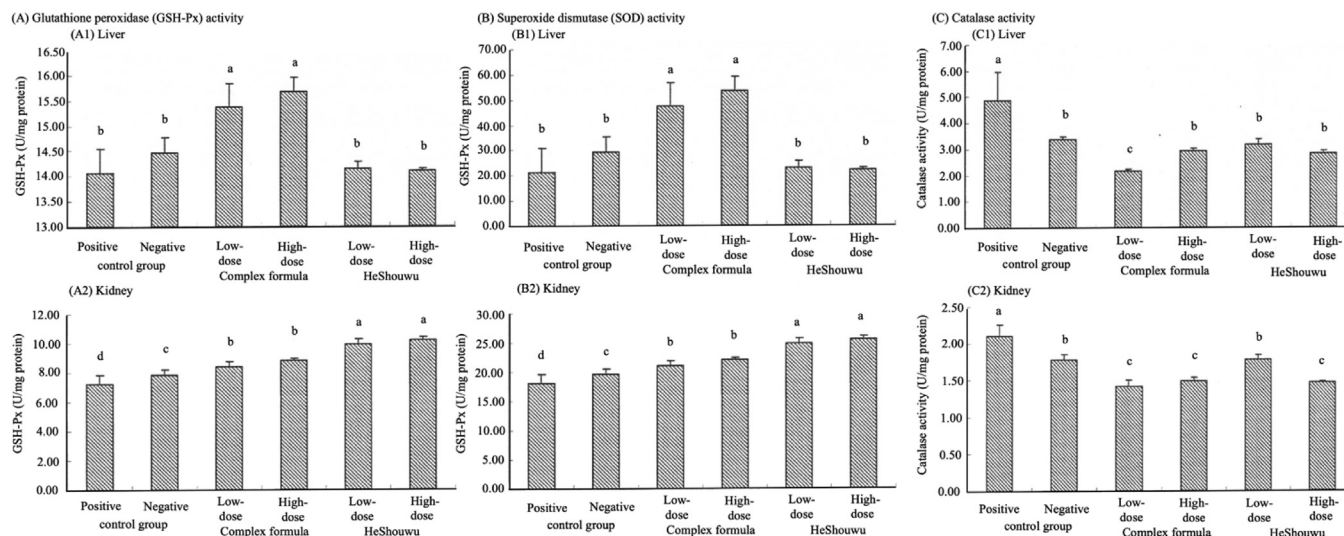


Fig. 2. Evaluation of antioxidant [glutathione peroxidase (GSH-Px), superoxide dismutase (SOD), catalase (CAT)] activities in the liver and kidney of hamsters fed with HeShouWu (*Polygonum multiflorum*) and its complex formula, positive and negative control groups. $n = 10$. Means with different letters are significantly different ($p < 0.05$).

ences compared to the other groups ($p < 0.05$) (Fig. 2A2). Notably, GSH-Px activity was higher in the negative control group than the positive control group, suggesting a self-repair response in the liver and kidney after inflammation, namely, producing more GSH-Px for antioxidation. However, Hu et al., (2021) reported that emodin, an active substance in HeShouWu, may affect cytochrome P450 metabolism, GSH metabolism, and steroid hormone biosynthesis, thereby causing hepatotoxicity. Teka et al., (2021) also reported similar findings. In particular, the emodin-GSH and the emodin-cysteine combinations result in abnormal lipid metabolism, amino acid metabolism, and bile metabolite excretion. Therefore, we hypothesized that the kidney was subjected to the metabolic competition described above, resulting in low GSH-Px activity in the HeShouWu groups.

Liver SOD activity was maximum in the low-dose HeShouWu group, and was significantly higher than the others ($p < 0.05$) (Fig. 2B1). However, higher activity was detected in the negative control group than in the positive control group, related to the self-repairing stress response in liver cells during inflammation. Similar results were found for kidney SOD activity, where the low-dose HeShouWu group had significantly higher SOD activity ($p < 0.05$) (Fig. 2B2). The positive control group exhibited significantly higher activity than the negative control group and the low-dose HeShouWu complex group ($p < 0.05$). However, emodin, a bioactive substance in HeShouWu, enhanced SOD activity while inhibiting MDA production and gene (GRP78 and CHOP) expression, thereby reducing hepatocyte steatosis (Cai et al., 2023). Therefore, this result suggests that the bioactive components of HeShouWu reacted in the liver to produce higher SOD activity than in the kidney.

Liver and kidney CAT activities were significantly higher in the positive control group than in all other groups ($p < 0.05$) (Fig. 2C1 and C2). The lowest CAT activity was observed in the low-dose HeShouWu complex group, suggesting that HeShouWu and its complex may have an inhibitory effect on CAT activity. TSG is a bioactive component in HeShouWu that modulates gene (PPAR- α and CYP2E1) expression and increases the activities of CAT, SOD, and GSH, thereby reducing lipid peroxidation and OS in the liver (Xue et al., 2020).

Lipid peroxidation is a recognized mechanism of OS in animals caused by producing reactive oxygen species (ROS), which causes tissue damage (Valko et al., 2006, Aljutaily 2022). Liver MDA con-

tent was significantly higher in the negative control group than in the other groups ($p < 0.05$) (Table 4), indicating that the high-cholesterol diet increased the liver MDA content in the hamsters. However, the treatments of HeShouWu and its complex significantly reduced MDA content ($p < 0.05$), which was satisfactory in both complex groups and high doses of HeShouWu. In addition, the high and low-dose HeShouWu complex groups revealed the lowest kidney MDA contents compared to the other groups ($p < 0.05$) (Table 4), while serum MDA content exhibited good performance in both HeShouWu groups ($p < 0.05$) (Table 4). These results show that MDA content (liver, kidney, and plasma) decreased significantly in the hamsters, and the antioxidant markers increased significantly in response to treatment with HeShouWu and its complex (Samadi-Noshahr et al., 2021). Hu et al., (2021) reported significant dose-dependent increases in hepatocyte ROS levels in hepatic stem cells (L02 and HepaRG) treated with a HeShouWu extract. However, this extract was cytotoxic at the maximum dose (2.5 mg/mL). Interestingly, MDA content in the treatment groups was lower than that in the positive control group with the stable OS, while HeShouWu and its complex might have multiplicative effects on autologous OS in the liver and serum. Thus, antioxidant (such as SOD, CAT, or GSH-Px) activities were activated by natural substances and autologous redox homeostasis, which protects the organism against OS (Valko et al., 2007, Akbulut et al., 2022, Aljutaily 2022, Barakat et al., 2022).

Thiols as biological mercaptans (R-SH, also called biothiols) significantly coordinate antioxidant defense networks (Sen and Packer 2000, Erel and Neselioglu 2014, Abdulsamed et al., 2021). They provide cellular (internal and external) antioxidant defense in the form of low molecular weight disulfides, such as homocysteine, cystine glycine, cystine, and GSSG (Rossi et al., 2009, Abdulsamed et al., 2021). Total thiols are powerful antioxidant agents that act as electron acceptors to oxidatively reduce unstable free radicals, maintain protein structure, and protect cells against OS-induced damage (Abdulsamed et al., 2021, Garavaglia et al., 2022). Therefore, changes in cellular thiol content have been used for regular clinical diagnosis and monitoring of various diseases involving OS and metabolic disorders (Erel and Neselioglu 2014, Chou et al., 2022). Total thiol contents in the liver and kidney were the highest in the low-dose HeShouWu group (liver) and the low-dose HeShouWu complex group (kidney), which both were significantly different than the others ($p < 0.05$) (Table 4). Yazdi et al.,

(2019) reported that total liver thiols are significantly lower in diabetic rats than in a control group, while total liver thiols increased significantly in all treatment groups compared with the diabetic group, which agreed with the present study. Samadi-Noshahr et al., (2021) also reported significantly higher total liver thiol contents in diabetic rats treated with fennel seed extract, *trans*-anethole (both at 400 mg/kg), or metformin (300 mg/kg), albeit a similar trend was observed in this study.

However, no dose-dependent relationship was observed in the increase of total liver thiol content in the HeShouWu treatment groups. Minimally invasive methods have been used to determine the levels of antioxidant enzymes or OS end-products (such as total thiols and native thiols) in the liver to assess the extent of OS (Akbulut et al., 2022). In addition, the accumulation of antioxidants in different areas of the same liver varies, while the thiol content of a tumor differs considerably compared to distant tissues (Koc et al., 2023). Moreover, Zinellu et al., (2010) reported that high plasma levels of thiols (LDL-S-homocysteine and glutamyl-cysteine) might be critical markers of excess cardiovascular disease risk in patients with CKD, which agreed with the findings of this study. However, several studies have reported decreased levels of total thiols in patients with moderate to severe CKD or in those on peritoneal dialysis as measured by the Ellman DTNB method (Himmelfarb et al., 2000, Prakash et al., 2004, Pieniazek et al., 2018, Garavaglia et al., 2022). HeShouWu and its complex alleviated plasma hyperlipidemia caused by excess cholesterol intake. However, the effect on the fatty liver was insignificant. A more intensive evaluation may be possible after a long examination period (>24 weeks) or a maximum dose (3-folds) (Liu et al., 2019) in the future.

4. Conclusions

In this study, He Shou Wu and its complexes reduced serum lipid levels in an animal model of hyperlipidemia induced by excess cholesterol intake with satisfactory effects. Despite slightly suppressing appetite (feed efficiency decreased to 0.045–0.053), the BW of the mice was not affected. However, HeShouWu and its complex facilitated the metabolism of cholesterol in the form of bile acids (451.5–484.4 µg/g feces) and reduced serum and liver lipids (TG and TC levels). Interestingly, the antioxidant potential of HeShouWu and its complex reduced the OS of cells and rebalanced redox homeostasis, despite the fat accumulation findings on the liver pathological sections. The study has demonstrated significant wellness-promoting benefits of HeShouWu and its complex.

Declaration of Competing Interest

The authors declare that they have no known competing financial interests or personal relationships that could have appeared to influence the work reported in this paper.

Acknowledgments

This research was financially supported by Taichung Veterans General Hospital/Providence University Joint Research Program (TCVGH-PU1128102) and Rong Sing Medical Foundation, Taiwan. This research was also supported by grants provided by the Ministry of Science and Technology (MOST 111-2313-B-126-002) in Taiwan.

References

Abdulsamed, K., G. Volkan, B. Ömer Faruk, et al., 2021. Thiols: Role in oxidative stress-related disorders. *Accenting Lipid Peroxidation*. A. Pinar. Rijeka, IntechOpen.

Adnan, M., Rasul, A., Hussain, G., et al., 2021. Physcion and physcion 8-O-β-D-glucopyranoside: Natural anthraquinones with potential anticancer activities.

Curr. Drug Targets 22, 488–504. <https://doi.org/10.2174/1389450121999201013154542>.

Aebi, H., 1984. [13] Catalase in vitro. *Methods in Enzymology*, Academic Press. 105: 121–126.

Aitken, A., Learmonth, M., 2009. Estimation of disulfide bonds using Ellman's reagent. In: Walker, J.M. (Ed.), *The Protein Protocols Handbook*. Press, Totowa, NJ, Humana, pp. 1053–1055.

Akbulut, S., Uremis, M.M., Sarici, K.B., et al., 2022. Measurement of oxidant and antioxidant levels in liver tissue obtained from patients with liver transplantation: A case-control study. *Transpl. Immunol.* 75. <https://doi.org/10.1016/j.trim.2022.101697> 101697.

Aljutaily, T., 2022. Evaluating the nutritional and immune potentiating characteristics of unfermented and fermented turmeric camel milk in cyclophosphamide-induced immunosuppression in rats. *Antioxidants* 11, 792.

Barakat, H., Alkabeer, I.A., Aljutaily, T., et al., 2022. Phenolics and volatile compounds of fennel (*Foeniculum vulgare*) seeds and their sprouts prevent oxidative DNA damage and ameliorates CCl4-induced hepatotoxicity and oxidative stress in rats. *Antioxidants* 11, 2318. <https://doi.org/10.3390/antiox11122318>.

Barakat, H., Alshimali, S.I., Almutairi, A.S., et al., 2022. Antioxidative potential and ameliorative effects of green lentil (*Lens culinaris* M.) sprouts against CCl4-induced oxidative stress in rats. *Front. Nutr.* 9. <https://doi.org/10.3389/fnut.2022.1029793>.

Brasil, B.B., Masaji, S., Martins, B.T., et al., 2022. Apolipoprotein C3 and circulating mediators of preadipocyte proliferation in states of lipodystrophy. *Mol. Metabol.* 64. <https://doi.org/10.1016/j.molmet.2022.101572> 101572.

Cai, M.-T., Zhou, Y., Ding, W.-L., et al., 2023. Identification and localization of morphological feature-specific metabolites in Reynoutria multiflora roots. *Phytochemistry* 206. <https://doi.org/10.1016/j.phytochem.2022.113527> 113527.

Chen, W., Wang, P., Chen, H., et al., 2021. The composition differences between small black beans and big black beans from different habitats and its effects on the processing of Polygonum multiflorum. *Phytochem. Anal.* 32, 767–779. <https://doi.org/10.1002/pca.3022>.

Cheng, C., Zhuo, S., Zhang, B., et al., 2019. Treatment implications of natural compounds targeting lipid metabolism in nonalcoholic fatty liver disease, obesity and cancer. *Int. J. Biol. Sci.* 15, 1654–1663. <https://doi.org/10.7150/ijbs.33837>.

Choi, R.-Y., Lee, M.-K., 2021. Polygonum multiflorum Thunb. hot water extract reverses high-fat diet-induced lipid metabolism of white and brown adipose tissues in obese mice. *Plants* 10, 1509.

Chou, M.-Y., Ho, J.-H., Huang, M.-J., et al., 2022. Potential antidepressant effects of a dietary supplement from the chlorella and lion's mane mushroom complex in aged SAMP8 mice. *Front. Nutr.* 9. <https://doi.org/10.3389/fnut.2022.977287>.

Dai, H.-Y., Chang, L.-S., Yang, S.-F., et al., 2023. HDAC6 promotes aggressive development of liver cancer by improving egfr mRNA stability. *Neoplasia* 35. <https://doi.org/10.1016/j.neo.2022.100845> 100845.

Drescher, H.K., Weiskirchen, R., Fülöp, A., et al., 2019. The influence of different fat sources on steatohepatitis and fibrosis development in the western diet mouse model of non-alcoholic steatohepatitis (NASH). *Front. Physiol.* 10. <https://doi.org/10.3389/fphys.2019.00770>.

Erel, O., Neselioglu, S., 2014. A novel and automated assay for thiol/disulphide homeostasis. *Clin. Biochem.* 47, 326–332. <https://doi.org/10.1016/j.clinbiochem.2014.09.026>.

Eslam, M., Newsome, P.N., Sarin, S.K., et al., 2020. A new definition for metabolic dysfunction-associated fatty liver disease: An international expert consensus statement. *J. Hepatol.* 73, 202–209. <https://doi.org/10.1016/j.jhep.2020.03.039>.

Fang, Q.-L., Qiao, X., Yin, X.-Q., et al., 2023. Flavonoids from *Scutellaria amoena* C. H. Wright alleviate mitochondrial dysfunction and regulate oxidative stress via Keap1/Nrf2/HO-1 axis in rats with high-fat diet-induced nonalcoholic steatohepatitis. *Biomed. Pharmacother.* 158. <https://doi.org/10.1016/j.biopha.2022.114160> 114160.

Gao, S.-S., Sun, J.-J., Wang, X., et al., 2020. Research on the mechanism of qushi huayu decoction in the intervention of nonalcoholic fatty liver disease based on network pharmacology and molecular docking technology. *Biomed Res. Int.* 2020, 1704960. <https://doi.org/10.1155/2020/1704960>.

Garavaglia, M.L., Giustarini, D., Colombo, G., et al., 2022. Blood thiol redox state in chronic kidney disease. *Int. J. Mol. Sci.* 23, 2853.

Gu, W., Yang, M., Bi, Q., et al., 2020. Water extract from processed Polygonum multiflorum modulate gut microbiota and glucose metabolism on insulin resistant rats. *BMC Complement. Med. Ther.* 20, 107. <https://doi.org/10.1186/s12906-020-02897-5>.

He, X., Liu, J., Long, G., et al., 2021. 2,3,5,4'-Tetrahydroxystilbene-2-O-β-D-glucoside, a major bioactive component from Polygoni multiflori Radix (Heshouwu) suppresses DSS induced acute colitis in BALB/c mice by modulating gut microbiota. *Biomed. Pharmacother.* 137. <https://doi.org/10.1016/j.biopha.2021.111420> 111420.

Himmelfarb, J., McMonagle, E., McMenamin, E., 2000. Plasma protein thiol oxidation and carbonyl formation in chronic renal failure. *Kidney Int.* 58, 2571–2578. <https://doi.org/10.1046/j.1523-1755.2000.00443.x>.

Hu, Y.-H., Li, D.-K., Quan, Z.-Y., et al., 2021. Exploration of components and mechanisms of Polygoni Multiflori Radix-induced hepatotoxicity using siRNA-mediated CYP3A4 or UGT1A1 knockdown liver cells. *J. Ethnopharmacol.* 270. <https://doi.org/10.1016/j.jep.2021.113845> 113845.

Huang, P.-H., Lu, H.-T., Wang, Y.-T., et al., 2011. Antioxidant activity and emulsion-stabilizing effect of pectic enzyme treated pectin in soy protein isolate-

- stabilized oil/water emulsion. *J. Agric. Food Chem.* 59, 9623–9628. <https://doi.org/10.1021/jf202020t>.
- Huang, P.-H., Chiu, C.-S., Lu, W.-C., et al., 2022. Effect of compositions on physicochemical properties and rheological behavior of gelatinized adzuki-bean cake (Yokan). *LWT* 168, <https://doi.org/10.1016/j.lwt.2022.113870>.
- Ji, X., Shi, S., Liu, B., et al., 2019. Bioactive compounds from herbal medicines to manage dyslipidemia. *Biomed. Pharmacother.* 118, <https://doi.org/10.1016/j.biopha.2019.109338>.
- Jung, S., Son, H., Hwang, C.E., et al., 2020. The root of *Polygonum multiflorum* Thunb. alleviates non-alcoholic steatosis and insulin resistance in high fat diet-fed mice. *Nutrients* 12, 2353.
- Koc, S., Akbulut, S., Sarici, K.B., et al., 2023. Measurement of heavy metal and antioxidant-oxidant levels in tissues obtained from three different localizations of explant hepatectomy of patients with hepatocellular carcinoma. *Transpl. Proc.* <https://doi.org/10.1016/j.transproceed.2022.11.013>.
- Kong, M.J., Han, S.J., Kim, J.I., et al., 2018. Mitochondrial NADP⁺-dependent isocitrate dehydrogenase deficiency increases cisplatin-induced oxidative damage in the kidney tubule cells. *Cell Death Dis.* 9, 488. <https://doi.org/10.1038/s41419-018-0537-6>.
- Koperska, A., Wesołek, A., Moszak, M., et al., 2022. Berberine in non-alcoholic fatty liver disease — A review. *Nutrients* 14, 3459.
- Li, X., 2012. Improved pyrogallol autoxidation method: a reliable and cheap superoxide-scavenging assay suitable for all antioxidants. *J. Agric. Food Chem.* 60, 6418–6424. <https://doi.org/10.1021/jf204970r>.
- Li, P.-H., Lu, W.-C., Chan, Y.-J., et al., 2020. Extraction and characterization of collagen from sea cucumber (*Holothuria cinerascens*) and its potential application in moisturizing cosmetics. *Aquaculture* 515, <https://doi.org/10.1016/j.aquaculture.2019.734590>.
- Li, P.-H., Chan, Y.-J., Lu, W.-C., et al., 2020. Bioresource utilization of *djulius* (*Chenopodium formosanum*) biomass as natural antioxidants. *Sustainability* 12, 5926.
- Li, F., Zhang, T., He, Y., et al., 2020. Inflammation inhibition and gut microbiota regulation by TSG to combat atherosclerosis in ApoE^{-/-} mice. *J. Ethnopharmacol.* 247, <https://doi.org/10.1016/j.jep.2019.112232>.
- Lin, L., Hao, Z., Zhang, S., et al., 2020. Study on the protection of water extracts of *Polygonum Multiflori Radix* and *Polygoni Multiflori Radix Praeparata* against NAFLD and its mechanism. *J. Ethnopharmacol.* 252, <https://doi.org/10.1016/j.jep.2020.112577>.
- Lin, S., Huang, J., Wang, M., et al., 2020. Comparison of MAFLD and NAFLD diagnostic criteria in real world. *Liver Int.* 40, 2082–2089. <https://doi.org/10.1111/liv.14548>.
- Liu, Y., Wang, W., Sun, M., et al., 2019. *Polygonum multiflorum*-Induced Liver Injury: Clinical characteristics, risk factors, material basis, action mechanism and current challenges. *Front. Pharmacol.* 10, <https://doi.org/10.3389/fphar.2019.01467>.
- Liu, J., Zhao, Y.-T., Lu, W.-C., et al., 2023. Bioactive compounds in malanto (*Kalimeris indica*) leaves and their antioxidant characteristics. *Agriculture* 13, 211.
- Nie, L., Song, H., He, A., et al., 2016. Recent research progress in natural bioactive constituents against lipid metabolic diseases. *Curr. Top. Med. Chem.* 16, 2605–2624. <https://doi.org/10.2174/1568026616666160414124145>.
- Paul, R., Shit, S.C., Fovanna, T., et al., 2020. Realizing catalytic acetophenone hydrodeoxygenation with palladium-equipped porous organic polymers. *ACS Appl. Mater. Interfaces* 12, 50550–50565. <https://doi.org/10.1021/acsami.0c16680>.
- Pieniazek, A., Gwozdziński, L., Zbrog, Z., et al., 2018. Alterations in conformational state of albumin in plasma in chronic hemodialyzed patients. *PLoS One* 13, e0192268.
- Prakash, M., Upadhyaya, S., Prabhu, R., 2004. Protein thiol oxidation and lipid peroxidation in patients with uraemia. *Scand. J. Clin. Lab. Invest.* 64, 599–604. <https://doi.org/10.1080/00365510410002869>.
- Reiter, E.B., Escher, B.I., Siebert, U., et al., 2022. Activation of the xenobiotic metabolism and oxidative stress response by mixtures of organic pollutants extracted with in-tissue passive sampling from liver, kidney, brain and blubber of marine mammals. *Environ. Int.* 165, <https://doi.org/10.1016/j.envint.2022.107337>.
- Rossi, R., Giustarini, D., Milzani, A., et al., 2009. Cysteinylation and homocysteinylation of plasma protein thiols during ageing of healthy human beings. *J. Cell Mol. Med.* 13, 3131–3140. <https://doi.org/10.1111/j.1582-4934.2008.00417.x>.
- Samadi-Noshahr, Z., Hadjzadeh, M.-A.-R., Moradi-Marjaneh, R., et al., 2021. The hepatoprotective effects of fennel seeds extract and trans-Anethole in streptozotocin-induced liver injury in rats. *Food Sci. Nutr.* 9, 1121–1131. <https://doi.org/10.1002/fsn3.2090>.
- Sen, C.K., Packer, L., 2000. Thiol homeostasis and supplements in physical exercise. *Am. J. Clin. Nutr.* 72, 653s–669s. <https://doi.org/10.1093/ajcn/72.2.653s>.
- Senthilkumar, M., Amaresan, N., Sankaranarayanan, A., 2021. Estimation of superoxide dismutase (SOD). In: Senthilkumar, M., Amaresan, N., Sankaranarayanan, A. (Eds.), *Plant-Microbe Interactions: Laboratory Techniques*. New York, NY, Springer, US, pp. 117–118.
- Senthilkumar, M., N. Amaresan and A. Sankaranarayanan, 2021. Estimation of malondialdehyde (MDA) by thiobarbituric Acid (TBA) assay. *Plant-Microbe Interactions: Laboratory Techniques*. M. Senthilkumar, N. Amaresan and A. Sankaranarayanan. New York, NY, Springer, US: 103–105.
- Simpson, R. J., 2010. Homogenization of mammalian tissue. *Cold Spring Harb Protoc.* 2010, pdb.prot5455. <https://doi.org/10.1101/pdb.prot5455>.
- Singh, S.P., Sashidhara, K.V., 2017. Lipid lowering agents of natural origin: An account of some promising chemotypes. *Eur. J. Med. Chem.* 140, 331–348. <https://doi.org/10.1016/j.ejmech.2017.09.020>.
- Teka, T., Wang, L., Gao, J., et al., 2021. *Polygonum multiflorum*: Recent updates on newly isolated compounds, potential hepatotoxic compounds and their mechanisms. *J. Ethnopharmacol.* 271, <https://doi.org/10.1016/j.jep.2021.113864>.
- Valko, M., Rhodes, C.J., Moncol, J., et al., 2006. Free radicals, metals and antioxidants in oxidative stress-induced cancer. *Chem. Biol. Interact.* 160, 1–40. <https://doi.org/10.1016/j.cbi.2005.12.009>.
- Valko, M., Leibfritz, D., Moncol, J., et al., 2007. Free radicals and antioxidants in normal physiological functions and human disease. *Int. J. Biochem. Cell Biol.* 39, 44–84. <https://doi.org/10.1016/j.biocel.2006.07.001>.
- Wang, C.-Y., Chen, Y.-W., Hou, C.-Y., 2019. Antioxidant and antibacterial activity of seven predominant terpenoids. *Int. J. Food Prop.* 22, 230–238. <https://doi.org/10.1080/10942912.2019.1582541>.
- Wang, W., He, Y., Lin, P., et al., 2014. In vitro effects of active components of *Polygonum Multiflorum Radix* on enzymes involved in the lipid metabolism. *J. Ethnopharmacol.* 153, 763–770. <https://doi.org/10.1016/j.jep.2014.03.042>.
- Wang, S., Yuan, R., Liu, M., et al., 2022. Targeting autophagy in atherosclerosis: Advances and therapeutic potential of natural bioactive compounds from herbal medicines and natural products. *Biomed. Pharmacother.* 155, <https://doi.org/10.1016/j.biopha.2022.113712>.
- Wang, L., Zhi, Y., Ye, Y., et al., 2020. Identify molecular mechanisms of Jiangzhi decoction on nonalcoholic fatty liver disease by network pharmacology analysis and experimental validation. *Biomed Res. Int.* 2020, 8829346. <https://doi.org/10.1155/2020/8829346>.
- Xiong, Q., Wilson, W.K., Pang, J., 2007. The liebermann–burchard reaction: sulfonation, desaturation, and rearrangement of cholesterol in acid. *Lipids* 42, 87–96. <https://doi.org/10.1007/s11745-006-3013-5>.
- Xu, X., Zhu, X.-P., Bai, J.-Y., et al., 2019. Berberine alleviates nonalcoholic fatty liver induced by a high-fat diet in mice by activating SIRT3. *FASEB J.* 33, 7289–7300. <https://doi.org/10.1096/fj.201802316R>.
- Xue, X., Quan, Y., Gong, L., et al., 2020. A review of the processed *Polygonum multiflorum* (Thunb.) for hepatoprotection: Clinical use, pharmacology and toxicology. *J. Ethnopharmacol.* 261, <https://doi.org/10.1016/j.jep.2020.113121>.
- Yazdi, H.B., Hojati, V., Shiravi, A., et al., 2019. Liver dysfunction and oxidative stress in streptozotocin-induced diabetic rats: Protective role of *Artemisia Turanica*. *J. Pharmacopunct.* 22, 109–114. <https://doi.org/10.3831/kpi.2019.22.014>.
- Ye, Q., Zou, B., Yeo, Y.H., et al., 2020. Global prevalence, incidence, and outcomes of non-obese or lean non-alcoholic fatty liver disease: a systematic review and meta-analysis. *Lancet Gastroenterol. Hepatol.* 5, 739–752. [https://doi.org/10.1016/S2468-1253\(20\)30077-7](https://doi.org/10.1016/S2468-1253(20)30077-7).
- Zahid, M.K., Sufian, H.B., Choudhury, M., et al., 2021. Role of macrophage autophagy in atherosclerosis: modulation by bioactive compounds. *Biochem. J.* 478, 1359–1375. <https://doi.org/10.1042/bcj20200894>.
- Zhang, P., Dong, X., Zhang, W., et al., 2023. Metabolic-associated fatty liver disease and the risk of cardiovascular disease. *Clin. Res. Hepatol. Gastroenterol.* 47, <https://doi.org/10.1016/j.clinre.2022.102063>.
- Zhou, H., Ma, C., Wang, C., et al., 2021. Research progress in use of traditional Chinese medicine monomer for treatment of non-alcoholic fatty liver disease. *Eur. J. Pharmacol.* 898, <https://doi.org/10.1016/j.ejphar.2021.173976>.
- Zhu, G., Chen, L., Liu, S., et al., 2022. Celecoxib-mediated attenuation of non-alcoholic steatohepatitis is potentially relevant to redistributing the expression of adiponectin receptors in rats. *Heliyon* 8, e09872.
- Zinellu, A., Loriga, G., Scanu, B., et al., 2010. Increased low-density lipoprotein S-Homocysteinylation in chronic kidney disease. *Am. J. Nephrol.* 32, 242–248. <https://doi.org/10.1159/000319012>.